Electronic Supplementary Material (ESI) for Analyst.

Highly catalysis amplification of MOF_{Nd}-loaded nanogold combined with specific aptamer SERS/RRS assay of trace glyphosate

Jingjing Li[a], Jinling Shi[a], Aihui Liang[a] and Zhiliang Jiang[a,*]

[a]Guangxi Key Laboratory of Environmental Pollution Control Theory and Technology, Key Laboratory of Ecology of Rare and Endangered Species and Environmental Protection (Guangxi Normal University), Ministry of Education, Guilin 541004, China.

*E-mail address: zljiang@mailbox.gxnu.edu.cn, ahliang2008@163.com

Contents

1. Additional Figures S1-S6

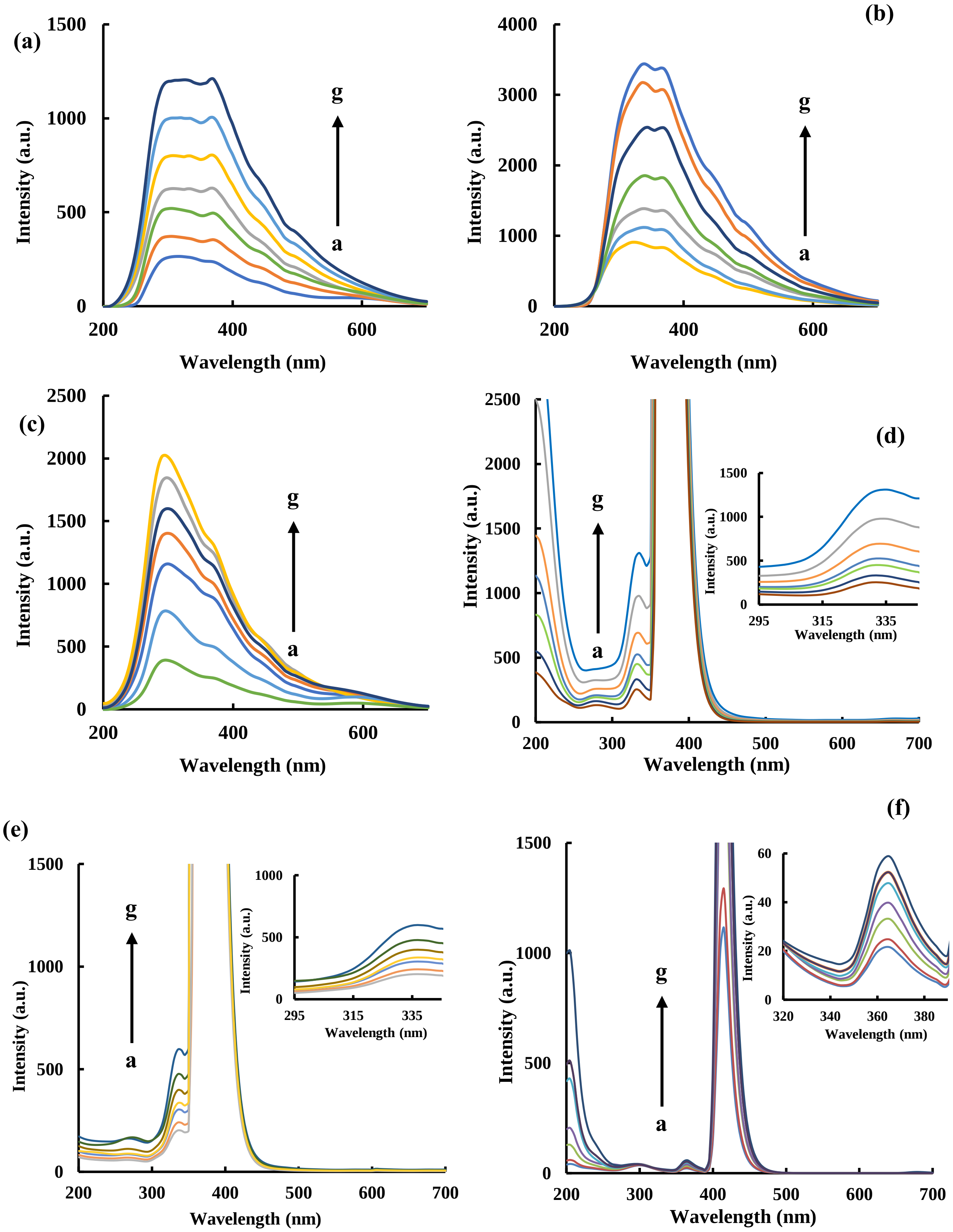

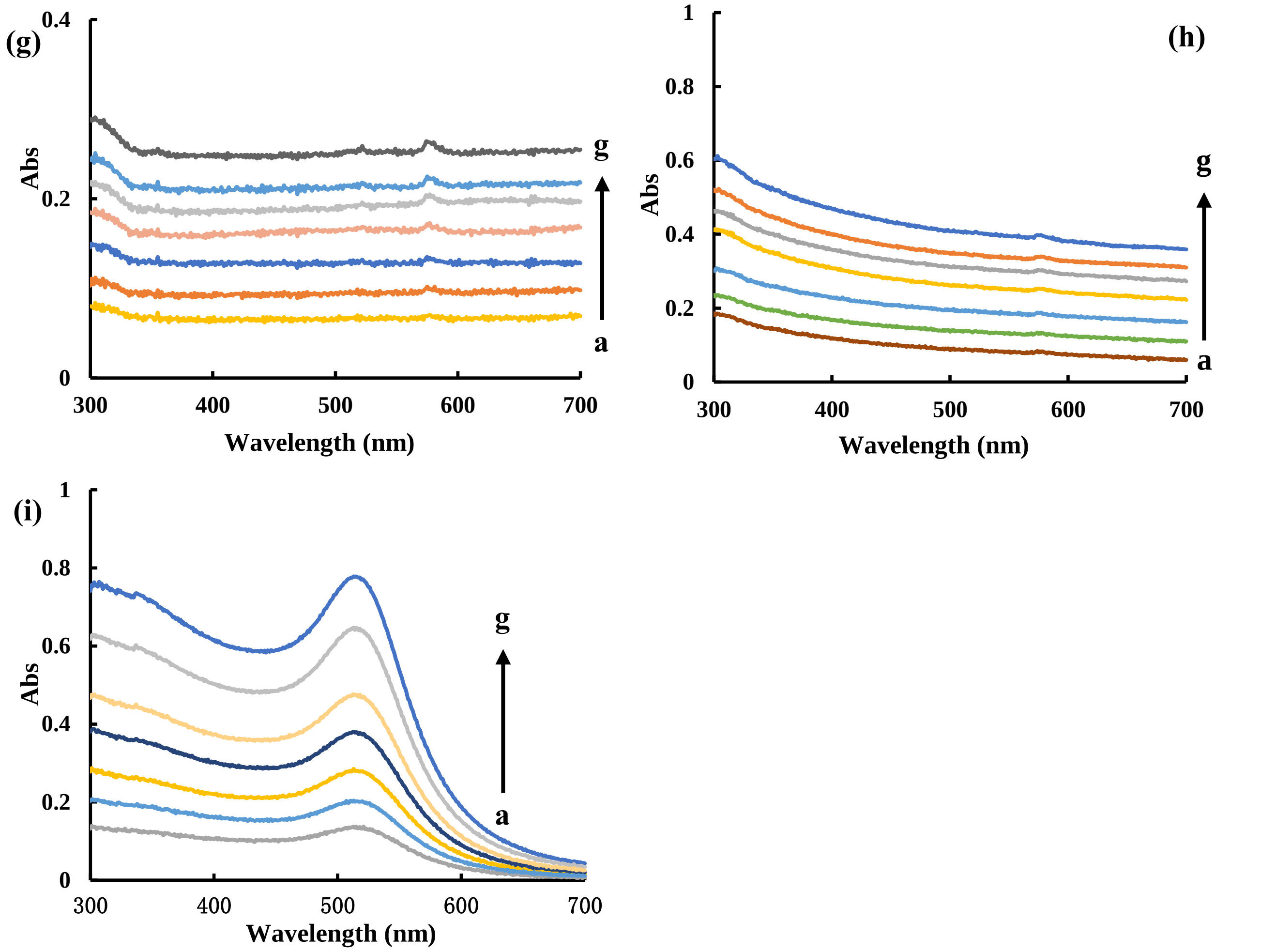

Figure S1 The RRS/Flu/Abs spectra of MOF_{Nd}/Au@MOF_{Nd}/$AuNP_B$: (a) RRS spectra of MOF_{Nd}, a–g: 25, 50, 100, 200, 300, 400, 500 μg mL^{-1} MOF_{Nd}. (b) RRS spectra of Au@MOF_{Nd}, a–g: 20, 30, 40, 50, 60, 70, 80 μg mL^{-1} Au@MOF_{Nd}. (c) RRS spectra of $AuNP_B$, a–g: 0.890, 1.78, 3.56, 7.13, 14.3, 28.5, 57.0 μg mL^{-1} $AuNP_B$. (d) Flu spectra of MOF_{Nd}, a–g: 25, 50, 100, 200, 300, 400, 500 μg mL^{-1} MOF_{Nd}. (e) Flu spectra of Au@MOF_{Nd}, a–g: 20, 30, 40, 50, 60, 70, 80 μg mL^{-1} Au@MOF_{Nd}. (f) Flu spectra of $AuNP_B$, a–g: 0.890, 1.78, 3.56, 7.13, 14.3, 28.5, 57.0 μg mL^{-1} $AuNP_B$. (g) Abs spectra of MOF_{Nd}, a–g: 25, 50, 100, 200, 300, 400, 500 μg mL^{-1} MOF_{Nd}. (h) Abs spectra of Au@MOF_{Nd}, a–g: 20, 30, 40, 50, 60, 70, 80 μg mL^{-1} Au@MOF_{Nd}. (i) Abs spectra of $AuNP_B$, a–g: 0.890, 1.78, 3.56, 7.13, 14.3, 28.5, 57.0 μg mL^{-1} $AuNP_B$.

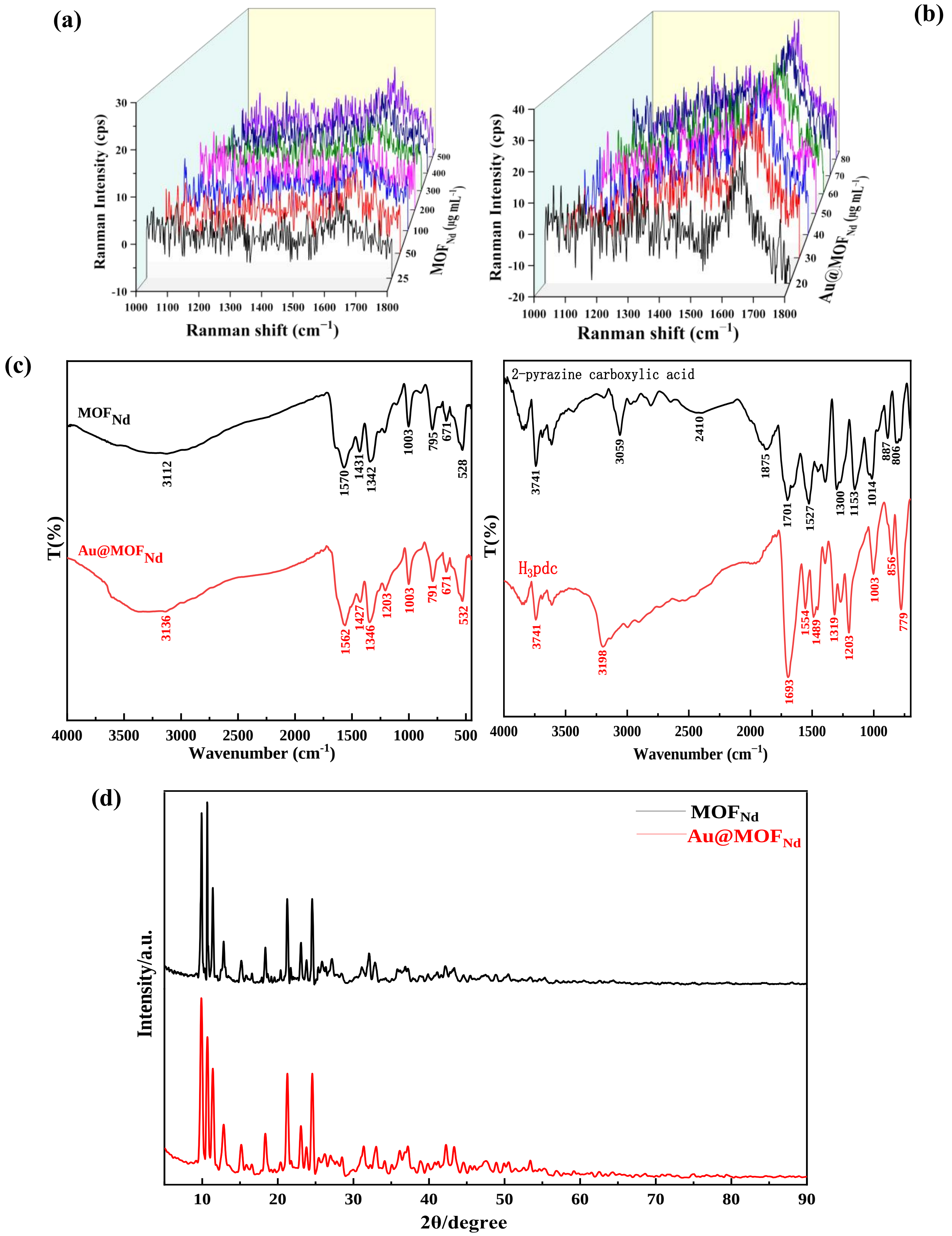

Figure S2 SERS/IR/XRD spectra of MOF_{Nd}/Au@MOF_{Nd}: (a) SERS spectrum of MOF_{Nd}, MOF_{Nd} + 80 nmol mL^{-1} AgNPs + 2.5 μmol mL^{-1} NaCl. (b) SERS spectrum of Au@MOF_{Nd}, Au@MOF_{Nd} + 80 nmol mL^{-1} AgNPs + 2.5 μmol mL^{-1} NaCl. (c) FTIR spectra of MOF_{Nd}, Au@MOF_{Nd}, 2−pyrazinecarboxylic acid and H_3pdc. (d) XRD of MOF_{Nd} and Au@MOF_{Nd}.

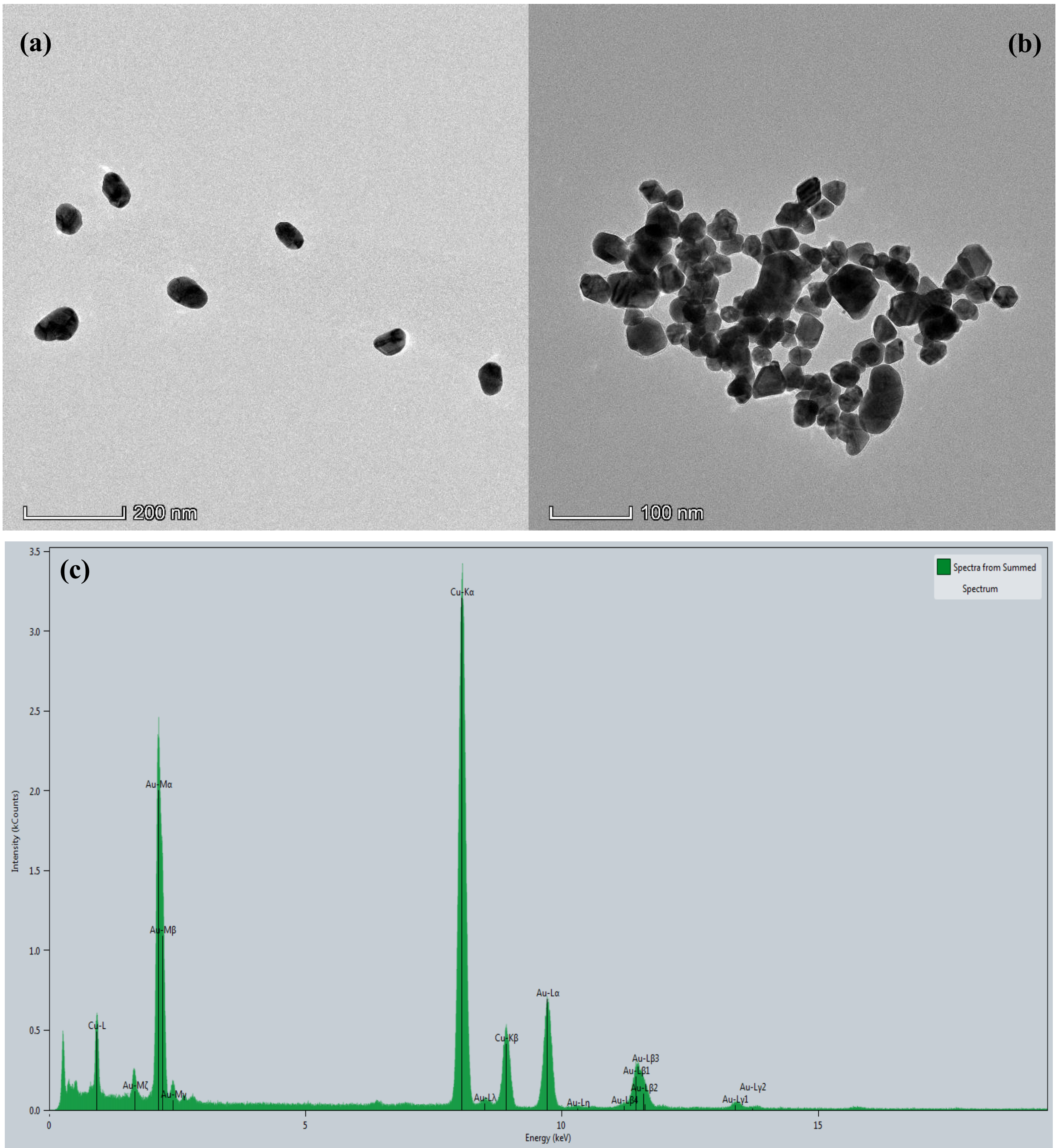

Figure S3 TEM and energy spectrum of the analysis system: (a) 8.75 nmol L^{-1} Apt_{GLY} + 5 ng mL^{-1} Au@MOF_{Nd} + 0.1 mmol L^{-1} Na_2SO_3 + 5.0×10^{-3} mmol L^{-1} $HAuCl_4$ + 0.5 mmol L^{-1} HCl. (b) a + 2 nmol L^{-1} GLY. (c) Energy spectrum of the analysis system.

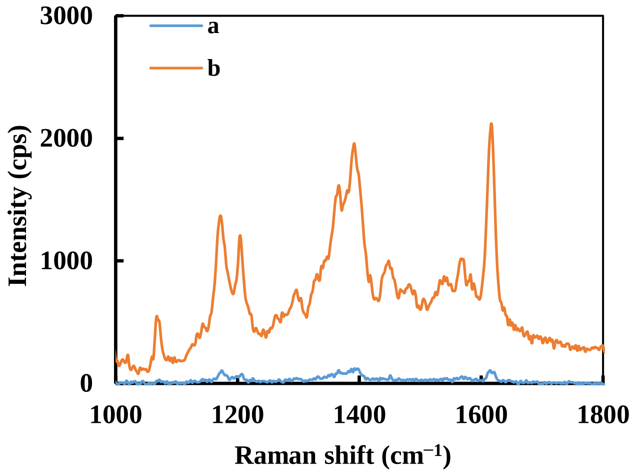

Figure S4 Normal Raman and SERS spectra of VB4r. (**a**) Normal Raman spectra of 0.1 mol L^{-1} VB4r solution. (**b**) SRES spectra of catalysis system: 5.0×10^{-3} mmol L^{-1} $HAuCl_4$ + 0.5 mmol L^{-1} HCl + 0.45 mmol L^{-1} Na_2SO_3 + 4.0 ng mL^{-1} Au@MOF_{Nd} + 0.25 μmol L^{-1} VB4r.

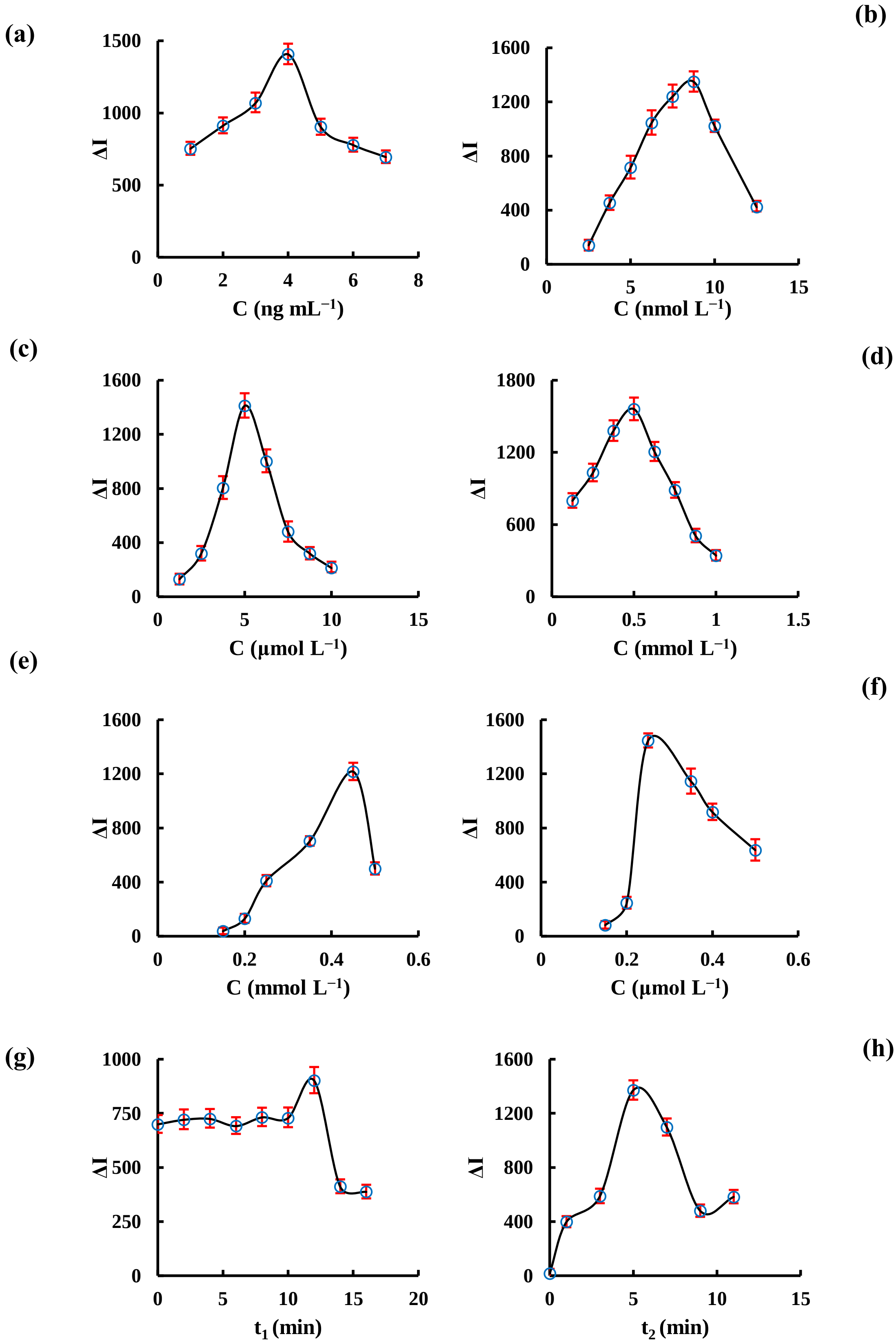

(a)
(b)
(c)
(d)
(e)
(f)
(g)
(h)
ΔI
C (ng mL⁻¹)
C (nmol L⁻¹)
C (μmol L⁻¹)
C (mmol L⁻¹)
C (mmol L⁻¹)
C (μmol L⁻¹)
t1 (min)
t2 (min)

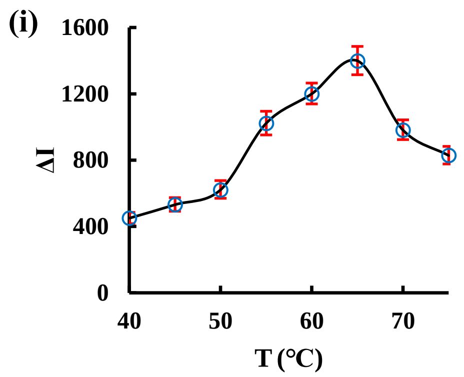

Figure S5 Optimization of SERS analysis conditions: (a) Au@MOF_{Nd} + 0.4 nmol L^{-1} GLY + 12.5 nmol L^{-1} Apt_{GLY} + 0.45 mmol L^{-1} Na_2SO_3 + 5.0 µmol L^{-1} $HAuCl_4$ + 0.5 mmol L^{-1} HCl + 0.25 µmol L^{-1} VB4r. (b) Apt_{GLY} + 0.4 nmol L^{-1} GLY + 4 ng mL^{-1} Au@MOF_{Nd} + 0.45 mmol L^{-1} Na_2SO_3 + 5.0 µmol L^{-1} $HAuCl_4$ + 0.5 mmol L^{-1} HCl + 0.25 µmol L^{-1} VB4r. (c) $HAuCl_4$ + 4 ng mL^{-1} Au@MOF_{Nd} + 0.4 nmol L^{-1} GLY + 10 nmol L^{-1} Apt_{GLY} + 0.45 mmol L^{-1} Na_2SO_3 + 0.5 mmol L^{-1} HCl + 0.25 µmol L^{-1} VB4r. (d) HCl + 10 nmol L^{-1} Apt_{GLY} + 0.4 nmol L^{-1} GLY + 4 ng mL^{-1} Au@MOF_{Nd} + 0.45 mmol L^{-1} Na_2SO_3 + 5.0 µmol L^{-1} $HAuCl_4$ + 0.25 µmol L^{-1} VB4r. (e) Na_2SO_3 + 10 nmol L^{-1} Apt_{GLY} + 0.4 nmol L^{-1} GLY + 4 ng mL^{-1} Au@MOF_{Nd} + 5.0 µmol L^{-1} $HAuCl_4$ + 0.5 mmol L^{-1} HCl + 0.25 µmol L^{-1} VB4r. (f) VB4r + 10 nmol L^{-1} Apt_{GLY} + 0.4 nmol L^{-1} GLY + 4 ng mL^{-1} Au@MOF_{Nd} + 0.45 mmol L^{-1} Na_2SO_3 + 5.0 µmol L^{-1} $HAuCl_4$ + 0.5 mmol L^{-1} HCl. (g) 10 nmol L^{-1} Apt_{GLY} + 0.4 nmol L^{-1} GLY + 4 ng mL^{-1} Au@MOF_{Nd} + 0.45 mmol L^{-1} Na_2SO_3 + 5.0 µmol L^{-1} $HAuCl_4$ + 0.5 mmol L^{-1} HCl + 0.25 µmol L^{-1} VB4r. (h) 10 nmol L^{-1} Apt_{GLY} + 0.4 nmol L^{-1} GLY + 4 ng mL^{-1} Au@MOF_{Nd} + 0.45 mmol L^{-1} Na_2SO_3 + 5.0 µmol L^{-1} $HAuCl_4$ + 0.5 mmol L^{-1} HCl + 0.25 µmol L^{-1} VB4r. (i) 10 nmol L^{-1} Apt_{GLY} + 0.4 nmol L^{-1} GLY + 4 ng mL^{-1} Au@MOF_{Nd} + 0.45 mmol L^{-1} Na_2SO_3 + 5.0 µmol L^{-1} $HAuCl_4$ + 0.5 mmol L^{-1} HCl + 0.25 µmol L^{-1} VB4r.

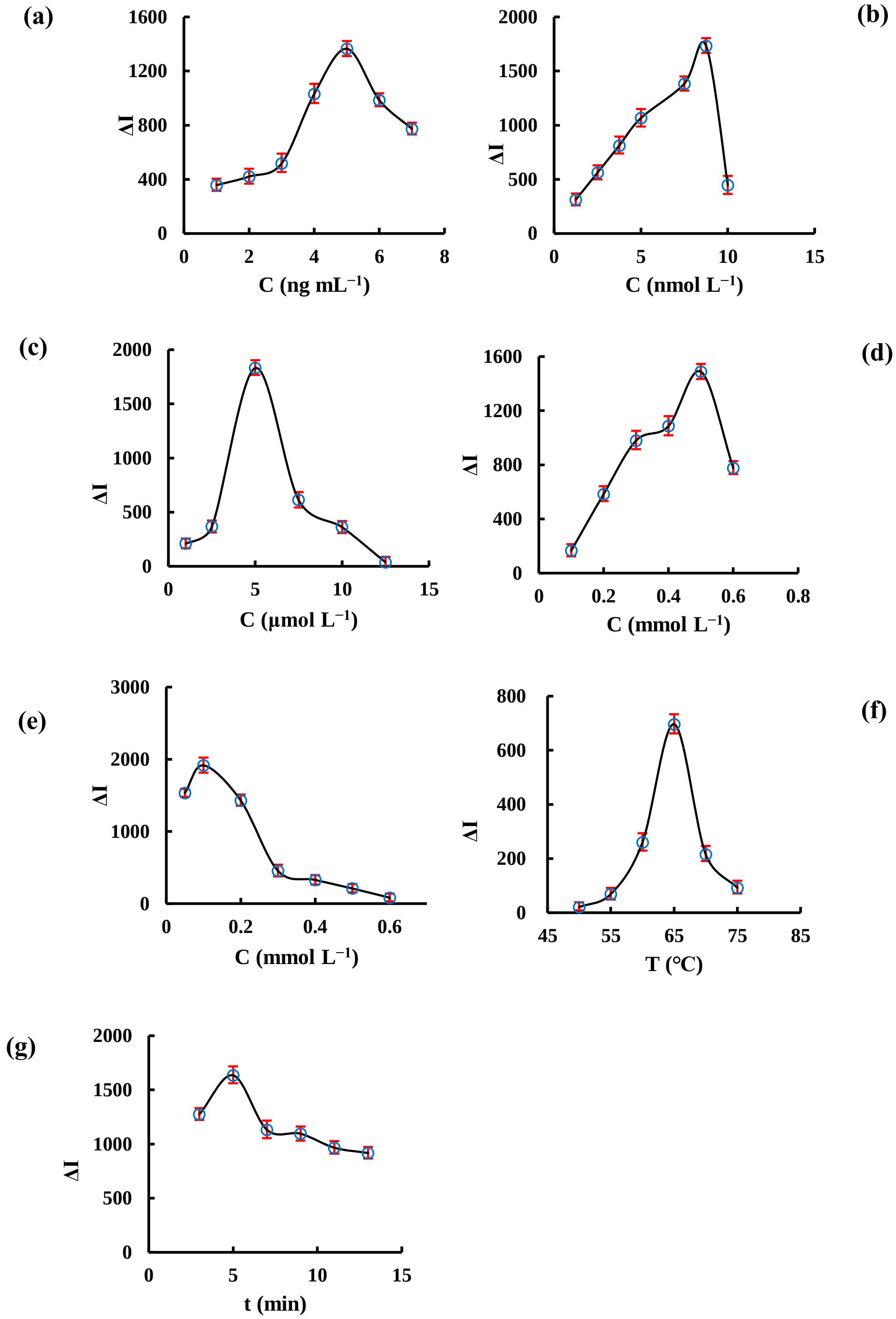

Figure S6 Optimization of RRS analysis conditions: (a) Au@MOF$_{Nd}$ + 5 nmol L^{-1} GLY + 10 nmol L^{-1} Apt$_{GLY}$ + 0.1 mmol L^{-1} Na_2SO_3 + 5.0 μmol L^{-1} $HAuCl_4$ + 0.5 mmol L^{-1} HCl. (b) Apt$_{GLY}$ + 5 nmol L^{-1} GLY + 5 ng mL^{-1} Au@MOF$_{Nd}$ + 0.1 mmol L^{-1} Na_2SO_3 + 5.0 μmol L^{-1} $HAuCl_4$ + 0.5

mmol L^{-1} HCl. (c) $HAuCl_4$ + 5 nmol L^{-1} GLY + 5 ng mL^{-1} Au@MOF_{Nd} + 8.75 nmol L^{-1} Apt_{GLY} + 0.1 mmol L^{-1} Na_2SO_3 + 0.5 mmol L^{-1} HCl. (d) HCl + 8.75 nmol L^{-1} Apt_{GLY} + 5 nmol L^{-1} GLY + 5 ng mL^{-1} Au@MOF_{Nd} + 0.1 mmol L^{-1} Na_2SO_3 + 5.0 µmol L^{-1} $HAuCl_4$. (e) Na_2SO_3 + 8.75 nmol L^{-1} Apt_{GLY} + 5 nmol L^{-1} GLY + 5 ng mL^{-1} Au@MOF_{Nd} + 5.0 µmol L^{-1} $HAuCl_4$ + 0.5 mmol L^{-1} HCl. (f) 8.75 nmol L^{-1} Apt_{GLY} + 5 nmol L^{-1} GLY + 5 ng mL^{-1} Au@MOF_{Nd} + 0.1 mmol L^{-1} Na_2SO_3 + 5.0 µmol L^{-1} $HAuCl_4$ + 0.5 mmol L^{-1} HCl. (g) 8.75 nmol L^{-1} Apt_{GLY} + 5 nmol L^{-1} GLY + 5 ng mL^{-1} Au@MOF_{Nd} + 0.1 mmol L^{-1} Na_2SO_3 + 5.0 µmol L^{-1} $HAuCl_4$.

2. Additional Tables S1-S4

Table S1 Catalytic effect of catalysts on $HAuCl_4$-Na_2SO_3 reaction

Catalyst	Linear range (ng mL^{-1})	Regression equation	Coefficient (R^2)
Au@MOF_{Nd}	1.0−7.0	ΔI_{1617} = 552.8 C + 3.8	0.9980
MOF_{Nd}	20−160	ΔI_{1617} = 7.0 C + 4.0	0.9943
$AuNP_B$	5.7−45.6	ΔI_{1617} = 33.1 C + 24.8	0.9970
$AuNP_C$	57−456	ΔI_{1617} = 3.1 C − 18.9	0.9984
AgNPs	8.6−68.8	ΔI_{1617} = 18.7 C − 21.0	0.9978

Table S2 Comparison of the reported GLY detection methods

Method	Principle	Linear range	Detection limit	Annotation	Reference
Electrochemical	Using luminol-Au-L-cysteine-Cu (II) composite as reagent, an electrochemical luminescence sensor was constructed to detect GLY.	0.001−1.0 μM	0. 5 nM	High sensitivity, complex preparation.	34
Fluorescence	Graphene quantum dot-Ag fluorescent probe was constructed to detect GLY.	30−2000 ng mL^{-1}	9 ng mL^{-1}	High sensitivity, high instrument cost	35
Fluorescence	A fluorescent method for GLY was developed by using Apt as probes.	0.1−10000 ng L^{-1}	88.80 ng L^{-1}	High sensitivity and complex operation	36
Colorimetry	A novel colorimetric nanozyme sheet was prepared based on Co_3O_4 nanosheets for detection of GLY.	/	0.175 mg kg^{-1}	Simple operation and low sensitivity.	37
TRES luminescence	Based on the specificity of Apt and luminescent G- quadruplex to construct a detection platform for GLY.	50−300 nM	26.4 nM	Low sensitivity and good selectivity	38
SPR spectrophotometry	A chitosan SPR sensor was constructed to detect GLY.	0−0.59 μM	8 nM	High reproducibility and low selectivity	39
SERS	A SERS method for GLY was established by Apt and catalytic amplification of COFs.	0.003−0.07 nM	0.002 nM	High sensitivity and complex catalyst preparation	40
SERS/RRS di-mode	Apt-mediated Au@MOF_{Nd} amplified SERS/RRS di-modal detection of GLY	0.05−0.5 nM 0.5−5.0 nM	0.02 nM 0.3 nM	High sensitivity and easy operation	this method

Table S3 The influence of interfering ions on the SERS system[a]

Coexisting substances	multiple	relative error (%)	Coexisting substances	multiple	relative error (%)
Mg^{2+}	100	2.1	HPO_4^{2-}	100	8.9
Fe^{3+}	1000	−5.4	$H_2PO_4^{-}$	100	−4.6
Ca^{2+}	100	8.2	$P_2O_7^{4-}$	1000	5.8
Al^{3+}	500	−2.2	NO_2^{-}	200	−4.7
Co^{2+}	500	6.1	CO_3^{2-}	500	5.2
Zn^{2+}	1000	4.6	L−Threonine	1000	−3.7
K^{+}	200	−2.3	L−Lysine	1000	−4.7
Cu^{2+}	500	−7.7	L−Histidine	100	3.1
HCO_3^{2-}	100	4.6	L−tryptophan	500	4.2
SO_3^{2-}	10	2.6	β− alanine	200	−2.4
SO_4^{2-}	10	1.3	Glycine	10	5.3

[a] 0.2 nmol L^{-1} GLY + 10 nmol L^{-1} Apt_{GLY} + 4 ng mL^{-1} $Au@MOF_{Nd}$ + 0.45 nmol L^{-1} Na_2SO_3 + 5.0×10^{-3} mmol L^{-1} $HAuCl_4$ + 0.5 mmol L^{-1} HCl + 0.25 μmol L^{-1} VB4r.

Table S4 SERS determination results of GLY in soil samples

sample	Single value (nM)	Average (nM)	Added (nM)	Found (nM)	Recovery (%)	RSD (%)	Content (μg g^{-1})
1	0.129 0.137 0.136 0.129 0.128	0.132	0.200	0.345	106.5	3.3%	0.178
2	0.128 0.130 0.122 0.121 0.118	0.124	0.200	0.321	98.5	4.1%	0.168
3	0.125 0.129 0.127 0.121 0.123	0.125	0.200	0.332	103.5	2.5%	0.169
4	0.143 0.138 0.141 0.146 0.140	0.142	0.200	0.328	93.0	2.2%	0.192

References

34 H. Liu, P. Chen, Z. Liu, J. Liu, J. Yi, F. Xia and C. Zhou, *Sens. Actuators B Chem.*, 2020, **304**, 127364.

35 J. Jiménez-López, E. J. Llorent-Martínez, P. Ortega-Barrales and A. Ruiz-Medina, *Talanta*, 2020, **207**, 120344.

36 M. Jiang, C. Chen, J. He, H. Zhang and Z. Xu, *Food Chem.*, 2020, **307**, 125534.

37 D. Luo, X. Huang, B. Liu, W. Zou and Y. Wu, *J. Agric. Food Chem.*, 2021, **69**, 3537–3547.

38 F. Chen, G. Li, H. Liu, C.-H. Leung and D.-L. Ma, *Sens. Actuators B Chem.*, 2020, **320**, 128393.

39 M. H. Do, B. Dubreuil, J. Peydecastaing, G. Vaca-Medina, T.-T. Nhu-Trang, N. Jaffrezic-Renault and P. Behra, *Sensors*, 2020, **20**, 5942.

40 Q. Liu, R. Zhang, B. Yu, A. Liang and Z. Jiang, *Sens. Actuators B Chem.*, 2021, **344**, 130288.